B. Lasorne and G. A. Worth (eds.)
Coherent Control of Molecules

Laser Control of Nuclear and Electron Dynamics: Bond Selective Photodissociation and Electron Circulation

Ingo Barth[a], Leticia González[a], C. Lasser[b], Jörn Manz[a] and Tamás Rozgonyi[c]
[a] *Institut für Chemie und Biochemie, Freie Universität Berlin, Takustrasse 3, 14195 Berlin, Germany*
[b] *Fachbereich Mathematik, Freie Universität Berlin, Arnimallee 6, 14195 Berlin, Germany*
[c] *Institute of Structural Chemistry, Chemical Research Center, Hungarian Academy of Sciences 1025 Budapest, Pusztaszeri út 59-67, Hungary*

I. INTRODUCTION

After the first fundamental approaches to quantum control of chemical reactions [1–4], the field has been developed to a powerful tool for driving reactants to specific products, beyond traditional chemical kinetics or photochemistry, see e.g. the reviews [5, 6] and the monografies [7, 8]. The early methods employed so-called "analytical" laser pulses which can be expressed by means of formulas with few parameters [1–3, 5–8]. Optimal control [2, 4, 9, 10], and further extensions to adaptive design of optimal laser pulses by means of feedback learning algorithms [11] have introduced much more flexible laser pulses, with myriads of parameters, stimulating the break-through [12] to impressive experimental applications [13–16]. Nevertheless, the original approaches based on analytical laser pulses remain useful, e.g. they may serve as a start, or reference for subsequent optimizations. Moreover, they allow rather easy interpretations of the underlying mechanism of laser control [1, 2, 5, 7, 8], in contrast with most applications of optimal laser pulses [12–15]; for an exception, see Ref. [16]. It remains an important task, therefore, to extend the previous approaches based on analytical laser pulses to new domains of applications.

The present paper demonstrates two extensions of quantum control based on analytical laser pulses: First, we shall apply the pump-dump approach of Tannor and Rice [17] to break preferably the stronger bond of a molecule, not the weaker one, for a new scenario where a single laser pulse would break either the weaker bond, or both. For this purpose, we shall design the laser driven path to selective bond-breaking, which may appear somewhat counter-intuitive, on first glance: The pump laser pulse excites the system to a transient highly excited electronic state which would induce double bond breaking. This impending disaster will

be turned into an advantage, however, i.e. preferential breaking of the strong bond, by means of the dump pulse.

Second, we present new aspects of extensions of quantum control, from nuclear to electron dynamics. Historically, the first example is the prediction [18] and experimental demonstration [19] of coherent control of uni-directional electron currents in solids by means of interfering one- plus two- or multi-photon excitations, analogous to coherent control of nuclear dynamics [1, 8]. Here, we investigate an alternative extension based on π pulses (cf. Refs. [3, 20, 21]) or $\pi/2$ pulses (cf. Refs. [22, 23]), in order to excite state-selective electronic ring currents [24] or electron circulation [25, 26] in ring-shaped molecules, respectively. For the previous quantum control of nuclear dynamics, we have designed efficient π or $\pi/2$ pulses with many cycles in the IR spectral domain, and with durations from few hundred fs to few ps, see also Refs. [5, 6, 23, 27, 28]; for early applications to non-reactive processes, see also the pioneering paper [29]. In contrast, analogous quantum control of electron dynamics calls for π or $\pi/2$ laser pulses with few cycles and with re-optimized parameters in the UV domain, and with durations from several hundred as to few fs [24–26], see also Refs. [21, 30]. Moreover, linear polarizations of the laser pulses [30] are extended to circularly polarized ones [24–26], see also Refs. [23, 31, 32]; for complementary applications of elliptically polarized or even arbitrary polarized pulses, see Refs. [14, 22, 33, 34]. Below, we shall focus on the condition [35]

$$\int_{-\infty}^{\infty} \underline{\mathcal{E}}(t)dt = 0 \tag{1}$$

for the extended applications of π or $\pi/2$ laser pulses with different shapes. This condition has been disregarded for traditional, rather long pulses because it is always fulfilled, at least as an excellent approximation, due to effects of cancellations of positive and negative contributions from electric fields with many cycles. However, these cancellations do not apply automatically for few cycle laser pulses, see e.g. Ref. [36]. Here we adapt the recipe of Bandrauk and coworkers [35] in order to design, exemplarily, few cycle $\pi/2$ pulses for electron circulation, in accord with the condition (1).

The two applications below, for extensions of pump-dump or $\pi/2$ laser pulses, assume that the molecules have been pre-oriented, e.g. by the methods of Ref. [37].

II. LASER CONTROL OF PHOTODISSOCIATION DYNAMICS

A popular target for coherent control is to maximize or minimize the branching between breaking a weak and strong bond in a polyatomic molecule. CH_2BrCl is a typical example where feedback learning algorithms [14] have demonstrated

an increase in the breaking of the strong C-Cl bond versus the weak C-Br one. Here, we investigate the efficiency of corresponding pump-dump laser pulses.

Our reduced model is composed of the three lowest singlet adiabatic potential energy surfaces (PES) along the two relevant $q_1 = d$(C-Cl) and $q_2 = d$(C-Br) reaction coordinates, as calculated in Refs. [38, 39]. The corresponding states a^1A', b^1A' and c^1A' are labelled 1, 2, 3, respectively, and in the Franck-Condon window they correspond to the n(Br)$\rightarrow \sigma^*$(C-Br) and n(Cl)$\rightarrow \sigma^*$(C-Cl) transitions. The b^1A' PES has two dissociation channels along the C-Br and C-Cl bond coordinates, but after vertical excitation the potential gradient favours C-Br dissociation. The c^1A' state allows double bond breaking, CH_2+X+Y, supported by transitions to the b^1A' state close to an avoided crossing near the line $q_1 \approx q_2$ [39].

The nuclear dynamics of the system is simulated with the time-dependent Schrödinger equation

$$i\hbar \begin{pmatrix} \dot{\Psi}_1 \\ \dot{\Psi}_2 \\ \dot{\Psi}_3 \end{pmatrix} = \begin{pmatrix} H_{11} & H_{12} & H_{13} \\ H_{21} & H_{22} & H_{23} \\ H_{31} & H_{32} & H_{33} \end{pmatrix} \cdot \begin{pmatrix} \Psi_1 \\ \Psi_2 \\ \Psi_3 \end{pmatrix}. \tag{2}$$

The time-dependent matrix elements of H_{ij} are in semiclassical dipole approximation written as $H_{ij}(t) = H^0_{ij} - \underline{d}_{ij} \cdot \underline{\mathcal{E}}(t)$. The molecular Hamiltonian H^0_{ij} contains the kinetic energy T, the adiabatic PES V, and the non-Born-Oppenheimer coupling, which as a first approximation is neglected. The coupling with the laser field $\underline{\mathcal{E}}(t)$ is described with the transition dipole operator $\underline{d}_{ij}$, here taken as $|d| = 0.5\, e a_0$ for each possible transition. The electric field comprises a pump-dump sequence $\underline{\mathcal{E}}(t) = \underline{\mathcal{E}}_p(t) + \underline{\mathcal{E}}_d(t)$ with time delay $t_{del} = t_p - t_d$, and each of the linearly polarized pulses ($l = p, d$) is given by

$$\underline{\mathcal{E}}_l(t) = \mathcal{E}_{0,l} \cos(\omega_l(t - t_l) + \eta_l) s_l(t - t_l) \underline{e}_l \tag{3}$$

where $\underline{e}_l, \mathcal{E}_{0,l}, \omega_l, \eta_l$ and t_l denote the polarization, the field amplitude, the carrier frequency, the phase, and the time of the peak maximum, respectively, and $\cos^2$ shape

$$s_l(t) = \cos^2(\pi t / t_{p,l}) \quad \text{for} \quad -t_{p,l}/2 \le t \le t_{p,l}/2, \tag{4}$$

with total pulse duration $t_{p,l}$. Phases η_l are set to zero for simplicity. The electric fields yield intensities $I_l(t) = \varepsilon_0 c |\underline{\mathcal{E}}_l(t)|^2$ ($l = 1, 2$) with peak values $I_{max,l} = \max I_l(t)$ and full width at half maximum (FWHM) τ_l, $I_l(\pm\tau_l/2) = I_{max,l}/2$. Averaging over the rapid (ω_l) cycles, $\overline{I_l(t)} = \varepsilon_0 c \overline{|\underline{\mathcal{E}}_l(t)|^2}$. The corresponding maximum intensities are then defined as $\overline{I_{max,l}} = \max \overline{I_l}(t) = 1/2 \varepsilon_0 c \mathcal{E}^2_{0,l}$.

Since the Franck-Condon region lies entirely in the $q_1 < q_2$ side, an excitation resonant to state b^1A' results exclusively in C-Br bond breaking, in accordance with experiments and chemical intuition. In contrast, a pump pulse resonant

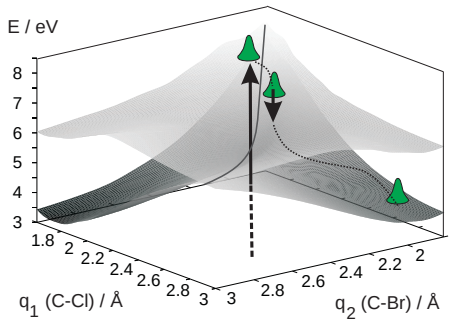

FIG. 1: Pump-dump control scenario for breaking the strong C-Cl bond of CH_2BrCl. The first, pump pulse creates a wave packet in the upper excited electronic state, which evolves in time (black dotted line). After crossing the $q_1 \approx q_2$ (solid) line, the second pulse dumps population to the lower excited electronic state, triggering dissociation of the target bond.

to the c^1A' state ($\hbar\omega_p$=7.17 eV, $t_{p,p}$=27.5 fs corresponding to 10 fs at FWHM, $\mathcal{E}_{0,p}$=3.89 GV/m, and peak intensity $\overline{I_{max,p}}$=2 TW/cm^2) creates a wave packet which crosses the avoided crossing line in the C-Cl direction, and then it turns to double dissociation CH_2 + Br + Cl, while broadening very quickly.

In order to maximize the fragmentation of the strong C-Cl bond we propose the pump-dump control scenario as shown schematically in Fig. 1: The *pump* pulse excites the molecule to the c^1A' state, and because of the shape of the PES (vide supra) the wave packet gets momentum in the C-Cl direction. After crossing the avoided crossing line $q_1 \approx q_2$, the *dump* or *control* pulse de-excites the system to the b^1A' state in the $q_2 < q_1$ region, where it dissociates towards C-Cl. This pump-dump mechanism profits from a "delicate" choice of the delay between both pulses. On one hand, the quick broadening of the wavepacket in the c^1A' state requires an early de-excitation, i.e. shortly after pumping. On the other hand, de-excitation should be late enough so that most of the wavepacket resides on the $q_2 < q_1$ side of the crossing line and with a dominant momentum still in the C-Cl direction and not yet along the $q_1 \approx q_2$ line, i.e. the appropriate position and momentum is obtained. As a compromise out of this dilemma, we use a very short dump pulse with optimal timing.

The optimized pump-dump pulse sequence and the time evolution of the populations in the corresponding states are shown in Fig. 2. The frequency of the dump pulse, $\hbar\omega_d$=1.0 eV, has been determined after investigating the path of the center of mass of the single-pulse-excited wave packet in the state c^1A'. The duration of the dump pulse and the time delay between the pulses have been optimized to achieve maximal depumping in the region of the PES which leads to C-Cl dissociation. More specifically, we have searched for i) maximizing the depumping from b^1A' to c^1A', i.e. the maximum of $\tilde{P}_2/(\tilde{P}_2 + \tilde{P}_3)$, which calls for early dump, ii) maximizing the amount of dumped population which dissociates along the C-Cl coordinate; this is given by $\tilde{P}_2(q_1 > q_2)/\tilde{P}_2$, and calls for a later dump pulse, and iii) the control efficiency defined as the product $\tilde{P}_2/(\tilde{P}_2 + \tilde{P}_3) \cdot \tilde{P}_2(q_1 > q_2)/\tilde{P}_2 = \tilde{P}_2(q_1 > q_2)/(\tilde{P}_2 + \tilde{P}_3)$ for goals (i) and (ii). Here, $\tilde{P}_i$ $(i = 1, 2, 3)$ denote the asymptotic values of the time-dependent popu-

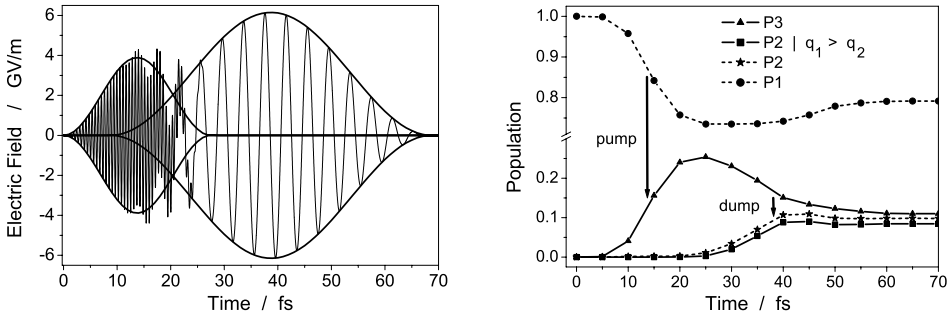

FIG. 2: The left figure shows the electric field for a pump pulse of $\hbar\omega_p$=7.17 eV, $t_{p,p}$=27.5 fs (FWHM = 10 fs), $\mathcal{E}_{0,p}$=3.89 GV/m, $\overline{I_{max,p}}$=2 TW/cm^2, and a dump or control pulse of $\hbar\omega_d$=1.0 eV, $t_{p,d}$=60 fs (FWHM = 22 fs), $\mathcal{E}_{0,p}$=6.15 GV/m, and $\overline{I_{max,d}}$=5 TW/cm^2. The time delay t_{del}=25 fs. The right figure shows the time-evolution of the populations of different electronic states. P_1, P_2 and P_3 are the populations of states a^{1}A', b^{1}A' and c^{1}A' respectively. $P_2|q_1 > q_2$ is the amount of P_2 which is on the $q_1 > q_2$ side of the crossing line, breaking the strong bond.

lations

$$P_i(t) = \int\int |\Psi_i(q_1, q_2, t)|^2 dq_1 dq_2 \tag{5}$$

integrated over all the space. Likewise,

$$P_2(q_1 > q_2) = \int\int |\Psi_2(q_1, q_2, t)|^2 dq_1 dq_2 \tag{6}$$

integrated for the domain $q_1 > q_2$ accounts for the fraction of the population P_2, which dissociates preferably to the C-Cl direction. The wave functions Ψ_i are normalized, so that $P_1(t) + P_2(t) + P_3(t) = 1$ for any time t .

Using these criteria (i)-(iii), we determine the optimal parameters of the dump pulse. For example, increasing the time delay from 20 fs to 30 fs, decreases the efficiency of depumping $\tilde{P}_2/(\tilde{P}_2 + \tilde{P}_3)$ but increases the ratio $\tilde{P}_2(q_1 > q_2)/\tilde{P}_2$. The optimum delay t_{del} is chosen at 25 fs. Likewise, depumping $\tilde{P}_2/(\tilde{P}_2 + \tilde{P}_3)$ increases but the ratio $\tilde{P}_2(q_1 > q_2)/\tilde{P}_2$ decreases with the duration of the dump pulse. The resulting laser parameters for the optimal compromise are listed in the Figure legend 2. With these parameters the overall depumped population, $\tilde{P}_2/(\tilde{P}_2 + \tilde{P}_3)$, measured at t=70 fs is 47.1 %, the portion of $\tilde{P}_2$ in the $(q_1 > q_2)$ region, $\tilde{P}_2(q_1 > q_2)/\tilde{P}_2$, is 86.2 % and the control efficiency $\tilde{P}_2(q_1 > q_2)/(\tilde{P}_2 + \tilde{P}_3)$ is 40.6 % (see Fig. 2).

In summary, we have shown that a pump-dump sequence can be tailored to induce significant fragmentation of a strong bond in a polyatomic molecule.

This is achieved by means of the apparent "detour" via the second excited state which would lead to double bond breaking, and optimal de-excitation to the first excited state which leads to the target product. Refinements of the model can be accomplished by including coordinate dependent transition dipole moments and non-adiabatic couplings. Moreover, the use of chirp [40], other polarizations, selective momentum along the C-Cl bond [41], or ultimately feedback controlled optimization [11] can certainly help improving the control yield.

III. LASER CONTROL OF ELECTRON DYNAMICS

In this section, laser control of nuclear dynamics is extended to electron dynamics for oriented molecules driven by (sub-)fs circularly polarized π or $\pi/2$ pulses. The right circularly polarized laser pulses propagating along the z-direction adapted from Refs. [24–26] may be rewritten as

$$\underline{\mathcal{E}}_1(t) = \mathcal{E}_{0,1} s_1(t) \begin{pmatrix} \cos(\omega_1 t + \eta_1) \\ \sin(\omega_1 t + \eta_1) \\ 0 \end{pmatrix} \tag{7}$$

with amplitude $\mathcal{E}_{0,1}$, carrier frequency ω_1, carrier envelope phase η_1, $\cos^2$ shape function denoted $s_1(t)$, equivalent to Eqn. (4), and duration $t_{p,1}$. For circularly polarized few cycle laser pulses (7), the condition (1) cannot be satisfied. According to Ref. [35], we suggest, therefore, a more flexible ansatz based on the vector potential $\underline{A}_2(t)$ such that the condition (1) is satisfied automatically,

$$\underline{A}_2(t) = -A_{0,2} s_2(t) \begin{pmatrix} \sin(\omega_2 t + \eta_2) \\ -\cos(\omega_2 t + \eta_2) \\ 0 \end{pmatrix} \tag{8}$$

with amplitude $A_{0,2} = c\mathcal{E}_{0,2}/\omega_2$. As shape function, we employ

$$s_2(t) = \cos^{20}(\pi t/t_{p,2}) \quad \text{for} \quad -t_{p,2}/2 \le t \le t_{p,2}/2 \tag{9}$$

which is very similar to a Gaussian [42], and therefore called "Gaussian" below. From expression (8), we derive the electric field $\underline{\mathcal{E}}_2(t) = -\underline{\dot{A}}_2(t)/c$

$$\underline{\mathcal{E}}_2(t) = \mathcal{E}_{0,2} s_2(t) \begin{pmatrix} \cos(\omega_2 t + \eta_2) \\ \sin(\omega_2 t + \eta_2) \\ 0 \end{pmatrix} + \frac{\mathcal{E}_{0,2}}{\omega_2} \dot{s}_2(t) \begin{pmatrix} \sin(\omega_2 t + \eta_2) \\ -\cos(\omega_2 t + \eta_2) \\ 0 \end{pmatrix} \tag{10}$$

For comparison of the results, we employ two laser pulses $\underline{\mathcal{E}}_1(t)$ and $\underline{\mathcal{E}}_2(t)$ with the same durations $\tau_E = \tau_{E,1} = \tau_{E,2}$ $(= \tau_1)$ of the squares of the envelopes $s_1(t)$ and $s_2(t)$, $s_k^2(\pm\tau_{E,k}/2) = 1/2$.

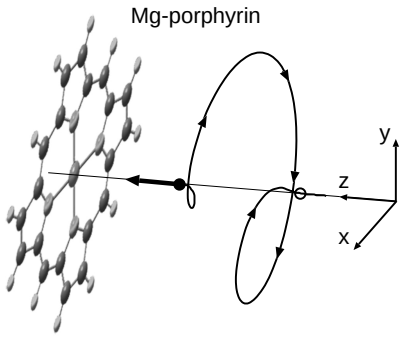

FIG. 3: Few cycle right circularly polarized laser pulse propagating along the z-direction (thick arrow) in order to induce the unidirectional right electron circulation in Mg-porphyrin, pre-oriented in the x/y-plane. The thin arrows indicate the time evolution of the electric field acting on the molecule, which appears clockwise ("right") when viewed along the z-direction of propagation, from $t = -2\,\mathrm{fs}$ ($\bullet$) to $t = 2\,\mathrm{fs}$ ($\circ$), compare Fig. 4.

Subsequently, we assume that the laser pulses are so short ($\tau_k < 1.5\,\mathrm{fs}$) that the nuclei are essentially frozen. The laser driven electron dynamics are then described by time-dependent electronic wave functions $|\Psi(t)\rangle$, solving the time-dependent Schrödinger equation in semiclassical dipole approximation

$$i\hbar|\dot{\Psi}(t)\rangle = H(t)|\Psi(t)\rangle = H_{el}|\Psi(t)\rangle - \underline{d}\cdot\underline{\mathcal{E}}_k(t)|\Psi(t)\rangle \tag{11}$$

where H_{el} denotes the electronic Hamiltonian, and $\underline{d}$ is the dipole operator.

Below, we apply laser pulses with intensities below the ionization thresholds ($I_{max.k} < 10\,\mathrm{TW/cm^2}$). The solution of Eqn. (11) may then be expanded in terms of electronic eigenstates $|\Psi_j\rangle$ with eigenenergies E_j.

$$|\Psi(t)\rangle = \sum_j C_j(t)|\Psi_j\rangle e^{-iE_j t/\hbar} \tag{12}$$

Insertion of the ansatz (12) into Eqn. (11) yields the equivalent set of equations for the time-dependent coefficients

$$i\hbar\dot{C}_j(t) = -\underline{\mathcal{E}}(t)\sum_i C_i(t)\langle\Psi_j|\underline{d}|\Psi_i\rangle e^{-i(E_i-E_j)t/\hbar} \tag{13}$$

The solutions $C_j(t)$ yield the populations $P_j(t) = |C_j(t)|^2$ of the levels E_j.

The subsequent application is for the laser pulse control of selective electron circulation in the ring-shaped molecule Mg-porphyrin (MgP) by means of a circularly polarized few cycle laser pulse, see Fig. 3.

The corresponding electronic eigenenergies and transition dipole matrix elements are taken from the literature [43, 44], as in Refs. [24–26]. Previously, we have designed various re-optimized π pulses of the type $\underline{\mathcal{E}}_1(t)$ in order to prepare the system in different excited state with E_{u+} (or E_{u-}) symmetry, and representing states with state selective right (or left) uni-directional ring currents [24]. These ring currents driven by laser pulses turn out to be much stronger,

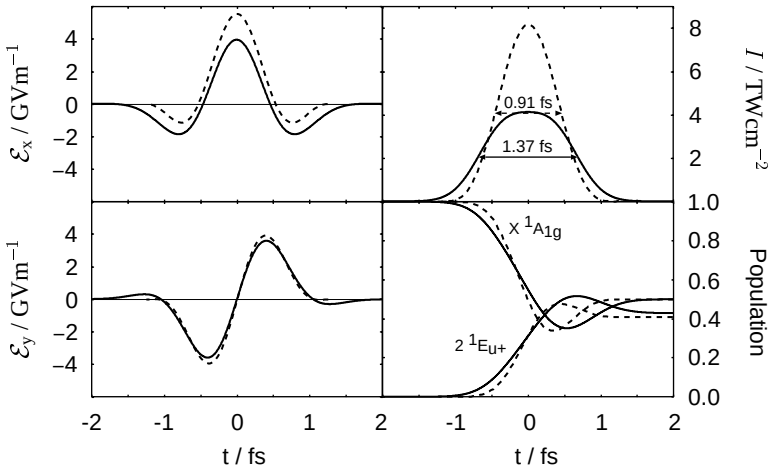

FIG. 4: Optimized circularly polarized laser pulses for half population transfer from the electronic ground state $X\,^1A_{1g}$ to excited target state $2\,^1E_{u+}$ implying state selective electron circulation in Mg-porphyrin. The figures show the x- and y-components of two electric fields $\underline{\mathcal{E}}_1(t)$ (Eqn. (7), dashed lines) and $\underline{\mathcal{E}}_2(t)$ (Eqn. (10), continuous lines), the corresponding intensities $I_1(t)$ and $I_2(t)$, and the resulting populations of the ground state $X\,^1A_{1g}$ and excited state $2\,^1E_{u+}$. The parameters of the laser pulse $\underline{\mathcal{E}}_1(t)$ and $\underline{\mathcal{E}}_2(t)$ are $\mathcal{E}_{0,1} = 5.54$ GVm^{-1}, $\hbar\omega_1 = 1.94$ eV, $\eta_1 = 0$ [25], and $\mathcal{E}_{0,2} = 3.94$ GVm^{-1}, $\hbar\omega_2 = 1.29$ eV, $\eta_2 = 0$, respectively. Note that, the FWHM of the squares of the envelopes $s_1(t)^2$ and $s_2(t)^2$ are the same for both pulses, $\tau_E = 0.91$ fs. In contrast, the FWHM of the intensities $I_1(t)$ and $I_2(t)$ are different, $\tau_1 = 0.91$ fs and $\tau_2 = 1.37$ fs.

e.g. 84.5 μA than traditional ones, i.e. one would need $B \approx 8000$ T in order to induce the same order of ring currents by permanent magnetic fields. Moreover, we have applied different re-optimized $\pi/2$ laser pulses $\underline{\mathcal{E}}_1(t)$ in order to prepare so-called "hybrid" superposition states

$$|\Psi_{i,j}(t)\rangle = 1/\sqrt{2}|\Psi_i\rangle e^{-i(E_i t/\hbar+\alpha_i)} + 1/\sqrt{2}|\Psi_j\rangle e^{-i(E_j t/\hbar+\alpha_j)} \qquad (14)$$

These are not eigenstates, i.e. they represent electron circulation, as demonstrated in Refs. [25, 26]. Below we apply the corresponding "Gaussian" laser pulse $\underline{\mathcal{E}}_2(t)$ with the same duration $\tau_E = \tau_{E,2} = \tau_{E,1}$ as for the $\cos^2$ shaped pulse $\underline{\mathcal{E}}_1(t)$. The optimal laser parameters are listed in the Figure legend 4, and the results for $\underline{\mathcal{E}}_2(t)$ are compared with those of $\underline{\mathcal{E}}_1(t)$ (adapted from Ref. [25]) in Fig. 4.

Accordingly, "Gaussian" laser pulses derived from corresponding ultra-short vector potential ($\tau_E = 910$ as) may be applied to induce state selective electron circulation in oriented ring-shaped molecules. This is advantageous because experimental "Gaussian" type laser pulse can be prepared more easily than $\cos^2$ shaped ones. Gratifyingly, the present effects of "Gaussian" laser pulses, which

satisfy condition (1) [35], confirm less rigorous previous results based on laser pulses with $\cos^2$ type shapes.

The present examples for exclusive quantum control of nuclear or electron dynamics point to a challenge, i.e. propagatation of the joint wave packet dynamics of electrons and nuclei driven by laser pulses, see e.g. Refs. [45, 46], with extended applications to quantum control.

Acknowledgement: JM would like to thank Prof. A. D. Bandrauk, Sherbrooke, for stimulating discussions of condition (1). Financial support by Berliner Förderprogramm (LG), Deutsche Forschungsgemeinschaft (project Ma 515/23-1), and Fonds der Chemischen Industrie (JM) are also gratefully acknowledged.

---

[1] P. Brumer and M. Shapiro, Chem. Phys. Lett. 126 (1986) 541.
[2] D. J. Tannor, R. Kosloff and S. A. Rice, J. Chem. Phys. 85 (1986) 5805.
[3] T. Joseph and J. Manz, Molec. Phys. 58 (1986) 1149.
[4] S. Shi, A. Woody and H. Rabitz, J. Chem. Phys. 88 (1988) 6870.
[5] J. Manz, in: Femtochemistry and Femtobiology: Ultrafast Reaction Dynamics at Atomic Scale Resolution, Nobel Symposium, ed. V. Sundström, vol. 101 (Imperial College Press, London, 1997) pp. 80–318.
[6] M. V. Korolkov, J. Manz and G. K. Paramonov, Adv. Chem. Phys. 101 (1997) 327.
[7] S. A. Rice and M. Zhao, Optical Control of Molecular Dynamics (Wiley, New York, 2000).
[8] M. Shapiro and P. Brumer, Principles of the Quantum Control of Molecular Processes (Wiley-VCH, Weinheim, 2003).
[9] R. Kosloff, S. A. Rice, P. Gaspard, S. Tersigni and D. J. Tannor, Chem. Phys. 139 (1989) 201.
[10] W. Jakubetz, J. Manz and H.-J. Schreier, Chem. Phys. Lett. 165 (1990) 100.
[11] R. S. Judson and H. Rabitz, Phys. Rev. Lett. 68 (1992) 1500.
[12] A. Assion, T. Baumert, M. Bergt, T. Brixner, B.Kiefer, V. Seyfried, M. Strehle and G. Gerber, Science 282 (1998) 919.
[13] R. J. Levis, G. M. Menkir and H. Rabitz, Science 292 (2001) 709.
[14] N. Damrauer, C. Dietl, G. Kramert, S.-H. Lee, K.-H. Jung and G. Gerber, Eur. Phys. J. D. 20 (2002) 71.
[15] T. Brixner and G. Gerber, Chem. Phys. Chem. 4 (2003) 418.
[16] C. Daniel, J. Full, L. González, C. Lupulescu, J. Manz, A. Merli, S. Vajda and L. Wöste, Science 299 (2003) 536.
[17] D. J. Tannor and S. A. Rice, J. Chem. Phys. 83 (1985) 5013.
[18] G. Kurizki, M. Shapiro and P. Brumer, Phys. Rev. B 39 (1989) 3435.
[19] E. Dupont, P. B. Corkum, H. C. Liu, M. Buchanan and Z. R. Wasilewski, Phys. Rev. Lett. 74 (1995) 3596.
[20] M. Sargent III, M. O. Scully and W. E. Lamb (Jr.), Laser Physics (Addison-Wesley,

London, 1974).
[21] J. Cao, C. J. Bardeen and K. R. Wilson, Phys. Rev. Lett. 80 (1998) 1406.
[22] Y. Fujimura, L. González, K. Hoki, D. Kröner, J. Manz and Y. Ohtsuki, Angew. Chem. Int. Ed. 39 (2000) 4586.
[23] K. Hoki, D. Kröner and J. Manz, Chem. Phys. 267 (2001) 59.
[24] I. Barth, J. Manz, Y. Shigeta and K. Yagi, J. Am. Chem. Soc. 128 (2006) 7043.
[25] I. Barth and J. Manz, Angew. Chem. Int. Ed. 45 (2006) 2962.
[26] I. Barth and J. Manz, in: Femtochemistry VII: A Conference Devoted to Fundamental Ultrafast Processes in Chemistry, Physics, and Biology, eds. J. A. W. Castleman and M. L. Kimble (Elsevier, Amsterdam, 2006) (in press).
[27] M. Holthaus and B. Just, Phys. Rev. A 49 (1994) 1950.
[28] L. González, D. Kröner and I. R. Solá, J. Chem. Phys. 115 (2001) 2519.
[29] G. K. Paramonov and V. A. Savva, Phys. Lett. A 97 (1983) 340.
[30] P. Krause, T. Klamroth and P. Saalfrank, J. Chem. Phys. 123 (2005) 074105.
[31] M. Kitzler, K. O'Keeffe and M. Lezius, J. Mod. Opt. 53 (2006) 57.
[32] S. X. Hu and L. A. Collins, Phys. Rev. A 73 (2006) 023405.
[33] Y. Fujimura, L. González, K. Hoki, J. Manz and Y. Ohtsuki, Chem. Phys. Lett. 310 (1999) 1, Corrigendium ibid 310 (1999) 578.
[34] L. Polachek, D.Oron and Y. Silberberg, Opt. Lett. 31 (2006) 631.
[35] S. Chelkowski and A. D. Bandrauk, Phys. Rev. A 71 (2005) 053815.
[36] N. Elghobashi, L. González and J. Manz, J. Chem. Phys. 120 (2004) 8002.
[37] H. Stapelfeldt and T. Seideman, Rev. Mod. Phys. 75 (2003) 543.
[38] L. González and T. Rozgonyi, J. Phys. Chem. A 106 (2002) 11150.
[39] L. González and T. Rozgonyi, J. Phys. Chem. A (2006), (in press).
[40] C. J. Bardeen, V. V. Yakovlev, K. R. Wilson, S. Carpenter, P. M. Weber and W. Warren, Chem. Phys. Lett. 280 (1997) 151.
[41] N. Elghobashi, P. Krause, J. Manz and M. Oppel, Phys. Chem. Chem. Phys. 5 (2003) 4806.
[42] I. Barth and C. Lasser (in preparation).
[43] M. Rubio, B. O. Roos, L. Serrano-Andrés and M. Merchán, J. Chem. Phys. 110 (1999) 7202.
[44] D. Sundholm, Chem. Phys. Lett. 317 (2000) 392.
[45] A. D. Bandrauk, S. Chelkowski and H. S. Nguyen, Int. J. Quant. Chem. 100 (2004) 834.
[46] G. K. Paramonov, Chem. Phys. Lett. 411 (2005) 350.